Selective CO Gas Detection of Zn_2SnO_4 Gas Sensor

JI HAENG YU & GYEONG MAN CHOI

Department of Materials Science and Engineering, Pohang University of Science and Technology, San 31, Hyoja-dong, Pohang 790-784, South Korea

Abstract. The ability of semiconductor gas sensors to differentiate between gases is essential but difficult to obtain. In this study, Zn_2SnO_4 was made to be CO selective and the possible mechanism for the selectivity was studied.

The electrical and the gas-sensing properties of uncoated and CuO-coated Zn_2SnO_4 were investigated. In order to obtain an ohmic contact to Zn_2SnO_4, a ZnO layer was stacked on top of Zn_2SnO_4 and co-fired. CuO was coated by immersing the sintered sample in Cu-containing solution. Both uncoated and CuO-coated samples showed the higher sensitivity to 200 ppm CO gas than to 200 ppm H_2 gas. However, the CuO-coated Zn_2SnO_4 showed much enhanced sensitivity and thus good selectivity for CO gas ($S_{CO}/S_{H_2} \sim 6$) compared to the uncoated sample. The excellent selectivity of Zn_2SnO_4-based materials for CO gas was explained by the difference in the mechanisms of CO and H_2 oxidation.

Keywords: zinc stannate, layered structure, gas sensor, selectivity

1. Introduction

The monitoring of carbon monoxide (CO) gas is essential since CO is not only a very toxic gas, but also a common gas produced by the incomplete combustion from factories, vehicles, and household appliances. Since SnO_2 was known as a good material to detect CO gas as well as other inflammable gases such as LPG and H_2 gas, a great deal of efforts have been focused on improving the performance of SnO_2-based gas sensors. The lack of gas selectivity for SnO_2 sensor, however, is a disadvantage as a semiconductor gas sensor [1]. Thus many studies focused on improving the selectivity and thus minimizing the interference by H_2 or C_2H_5OH gases in monitoring CO gas [2]. Noble metal catalysts such as Pd and Pt were widely used to improve the sensitivity and the selectivity to CO gas [3, 4]. It was also proposed that the heterogeneous interface between semiconductor oxides, e.g. ZnO(n)/CuO(p) [5, 6], is helpful to obtain the selectivity to CO gas. Mixture- [7–9] and layered-type [10–12] composite sensors were also proposed to improve the stability of interface.

In this study, Zn_2SnO_4 (zinc stannate) formed by the reaction between ZnO and SnO_2, was studied as a sensing material. Zn_2SnO_4 has been studied for the applications as transparent electrodes, window coatings, and gas sensors to detect i-C_4H_{10} [13], NO [14], NO_2 [15], and C_2H_5OH [16] gases. Previously, we have also found that Zn_2SnO_4 showed a high sensitivity to CO gas at low temperature ($\sim 240°C$) and a high sensitivity to H_2 gas at high temperature ($\sim 380°C$) [12]. It was not clear, however, why Zn_2SnO_4 showed good selectivity to CO gas without any additional catalysts. The observed selectivity was scarcely found in other semiconductor gas-sensing materials. In this study, we investigated the temperature dependence of sensitivity to CO and H_2 gases and discussed the possible sensing mechanism of CO gas-selective Zn_2SnO_4.

CuO was coated on the surface Zn_2SnO_4 in order to modify the gas-sensing properties of Zn_2SnO_4. CuO was known to lower the sensing temperature of SnO_{2-} and ZnO-based gas sensors [7, 17]. Thus it is expected that CuO-coated Zn_2SnO_4 may have an added advantage in the selective detection of CO gas. In order to characterize the electrical and

gas-sensing properties of Zn_2SnO_4, ZnO layer was stacked on top of Zn_2SnO_4 and co-fired. We have previously reported that Zn_2SnO_4 with Pt electrodes showed non-ohmic current-voltage (I-V) characteristics, especially in reducing atmosphere, possibly due to the electrical field-induced chemisorption of oxygen at $(-)Pt/Zn_2SnO_4(+)$ interface [18]. ZnO layer made the ohmic contact possible for Zn_2SnO_4 and thus the electrical and the gas-sensing properties of Zn_2SnO_4 were conveniently studied without interference from electrodes.

2. Experimental Procedure

Zn_2SnO_4 powder was synthesized by solid-state reaction. Commercial ZnO (Aldrich, USA, 99.9%) and SnO_2 powders (Aldrich, 99.9%) were mixed in 2:1 ratio by ball milling with zirconia balls in ethyl alcohol for 12 h followed by calcining at 1000°C for 3 h. It has been reported that intermediate compounds such as $ZnSnO_3$ and Zn_2SnO_4 can be made at lower temperatures by chemical mixing process [19]. In our system, however, only Zn_2SnO_4 phase was found by XRD [12].

In order to make the layered-type sample, 5 mol% SnO_2-added ZnO powder was also prepared by ball-milling the mixture of SnO_2 and ZnO powders. The addition of SnO_2 resulted in the formation of small amount of Zn_2SnO_4 phase in ZnO matrix and prevented the densification of ZnO when sintered above 1000°C. As a result, the porous ZnO phase made very stable contact with porous Zn_2SnO_4 after sintering. The conditions for the stable junction between two different oxides were described in detail elsewhere [10, 20]. Hereafter, we denote the 5 mol% SnO_2-added ZnO as ZnO for simplicity. Die-pressing ZnO powder on top of Zn_2SnO_4 powder made the green body of layered ZnO/Zn_2SnO_4. The amount of powder was controlled for each layer to have the same thickness after sintering. The green body was cold-isostatically pressed at 200 MPa and then sintered at 1000°C for 3 h. The sample had approximate dimension of $\sim$7.5 mm $(\phi) \times 3$ mm (t) after sintering.

CuO-coated sample was also made by immersing the sintered sample into 1 wt% CuO solution prepared by Pechini method [21] for 1 h. The CuO-impregnated sample was heated to 350°C for 2 h followed by firing at 750°C for 3 h. Provided that the pores of Zn_2SnO_4 ($\sim$40%) were fully filled with CuO solution, the residual amount of CuO after firing is estimated as $\sim$0.5 mol%.

For the electrical characterization, Pt paste (Engelhard model #6082) was painted on the flat surfaces of the samples followed by firing at 600°C for 30 min. Thus the layered samples had the structure of $Pt/ZnO/Zn_2SnO_4/Pt$. In order to avoid the interference by pre-adsorbed hydroxyl group (OH^-), the samples were heated to 450°C in air before cooling to the measurement temperature. CO and H_2 gases, 200 ppm balanced by air, were used to investigate the gas-sensing properties of samples. The relative humidity was fixed to 23% at 25°C by flowing the gases through the $MgCl_2$ saturated solution [22].

The current-voltage characteristics were measured after equilibrating the samples in air for 60 min and in reducing gas (200 ppm CO or 200 ppm H_2) for 20 min, respectively. Using high-voltage source/measure unit (Keithley, K237, USA), the current was measured 2 s after applying the bias voltage from -10 to 10 V to the samples. Before changing the measurement temperature, the samples were kept in air for 30 min in order to recover their electrical conductivities in air. Gas sensitivity is defined as the ratio of R_{Air}/R_{Gas}, where R_{Air} and R_{Gas} denote the resistance values measured in air and reducing atmosphere, respectively.

3. Results and Discussion

3.1. I-V Characteristics of ZnO/Zn₂SnO₄ Layered Sample

Figure 1 shows the current-voltage (I-V) characteristics of ZnO/Zn_2SnO_4 layered sample in contact with Pt ($Pt/ZnO/Zn_2SnO_4/Pt$) and Zn_2SnO_4 sample in contact with Pt ($Pt/Zn_2SnO_4/Pt$), in a reducing atmosphere
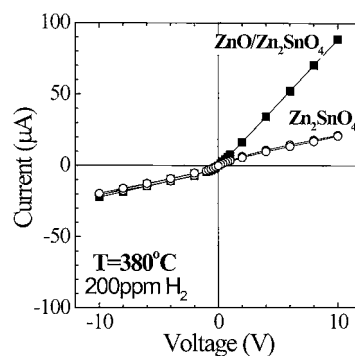

Fig. 1. Current-voltage characteristics of Zn_2SnO_4 and ZnO/Zn_2SnO_4 samples at 380°C in 200 ppm H_2.

(200 ppm H_2). For ZnO/Zn_2SnO_4 layered sample, forward bias was defined when Zn_2SnO_4 was positively biased $((-)Pt/ZnO/Zn_2SnO_4/Pt(+))$. Note that Zn_2SnO_4 sample in contact with Pt electrodes showed a symmetric non-linear $I\text{-}V$ curve while ZnO/Zn_2SnO_4 sample with asymmetric electrodes, i.e., Pt/ZnO on one side and Pt on the other side, showed an asymmetric curve. The $I\text{-}V$ curve of ZnO/Zn_2SnO_4 sample was nearly linear under forward bias as the non-ohmic contact of Zn_2SnO_4 sample, $(-)Pt/Zn_2SnO_4(+)$, was replaced with $(-)ZnO/ZnSnO_4(+)$ interface. The $I\text{-}V$ characteristics of the samples in 200 ppm CO were analogous to those shown in Fig. 1. The non-ohmic behavior of Zn_2SnO_4 has been explained by slowly increasing resistance of $(-)Pt/Zn_2SnO_4(+)$ interface due to electro-adsorption effect [18]. Thus the electrical and gas-sensing properties of Zn_2SnO_4 can be observed more clearly from the forward $I\text{-}V$ curves of ZnO/Zn_2SnO_4-layered sample. Accordingly, the electrical conductivity and the sensitivity to CO and H_2 gases of Zn_2SnO_4 were calculated from the $I\text{-}V$ curves under forward bias. CuO-coated ZnO/Zn_2SnO_4 sample also showed asymmetric $I\text{-}V$ characteristics although the deviation from linearity in reverse current was slightly reduced from that of uncoated (or 'undoped' as explained later) sample. Since the electrical characteristics of Zn_2SnO_4, either uncoated or CuO-coated, were obtained from the layered sample, hereafter, we denote the uncoated and CuO-coated ZnO/Zn_2SnO_4 layered samples as Zn_2SnO_4 and Zn_2SnO_4:Cu, respectively. The resistance of ZnO layer was too small to contribute to the electrical conductivity.

3.2. Electrical and Gas-Sensing Properties of Zn_2SnO_4 and Zn_2SnO_4:Cu

Electrical conductivities Zn_2SnO_4 and Zn_2SnO_4:Cu in air (23% R.H.) are plotted as a function of temperature in Fig. 2. The electrical conductivity of Zn_2SnO_4 was reduced by CuO addition. Several factors should be simultaneously considered to interpret the decreased conductivity with CuO coating. First, the possible change of microstructure with CuO addition was examined. With SEM microscopy, however, we could not find any noticeable difference between the microstructures of Zn_2SnO_4 and Zn_2SnO_4:Cu. The BET surface area of Zn_2SnO_4:Cu ($\sim 3.04 \pm 0.05\ m^2/g$) changed little from that of Zn_2SnO_4 ($\sim 3.00 \pm 0.06\ m^2/g$).
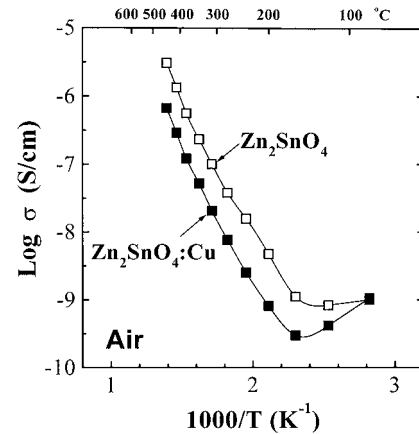

Fig. 2. Electrical conductivity of Zn_2SnO_4 and CuO-coated Zn_2SnO_4 (Zn_2SnO_4:Cu) samples in air (23% R.H.).

Although the CuO-impregnated body was fired again at 750°C, the firing temperature was much lower than the sintering temperature (1000°C). Secondly, the doping by aliovalent Cu^{+2} (or partly Cu^+) ions may have led to the reduced electrical conductivity. We have reported that the addition of CuO reduced the electrical conductivity of SnO_2 without any remarkable change in microstructure [17]. CuO addition also decreased the electrical conductivity of ZnO, which was explained by the substitutional doping effect of Cu^+ into Zn^{+2} ions [23]. Cu^{+2} and/or Cu^+ may have substituted Sn^{+4} and Zn^{+2} sites of Zn_2SnO_4 and lowered the electrical conductivity of n-type Zn_2SnO_4 as shown in Fig. 2. In conclusion, the decrease of conductivity with CuO coating is mostly due to the doping effect.

Sensitivities of Zn_2SnO_4 and Zn_2SnO_4:Cu were calculated from the forward $I\text{-}V$ curves and plotted as a function of temperature as shown in Figs. 3(a) and (b), respectively. Zn_2SnO_4 sample showed the maximum sensitivity to 200 ppm H_2 at $\sim 410°C$ while to 200 ppm CO gas at lower temperature ($\sim 350°C$). Note that the sensitivity curve for CO gas is broader than that for H_2 gas. As a result, Zn_2SnO_4 showed higher sensitivity to CO gas (~ 3) at 240°C than to H_2 gas (~ 1) although the maximum sensitivity to CO gas (~ 8 at 350°C) was less than that to H_2 gas (~ 15 at 410°C). Thus, Zn_2SnO_4 sample showed the selectivity to CO gas against H_2 gas below $\sim 300°C$ as shown in Fig. 4. The CO-gas selectivity was defined as the ratio of the CO-gas sensitivity to the H_2-gas sensitivity, S_{CO}/S_{H_2}. The possible mechanism of selective detection of CO gas was discussed in detail in the following section.

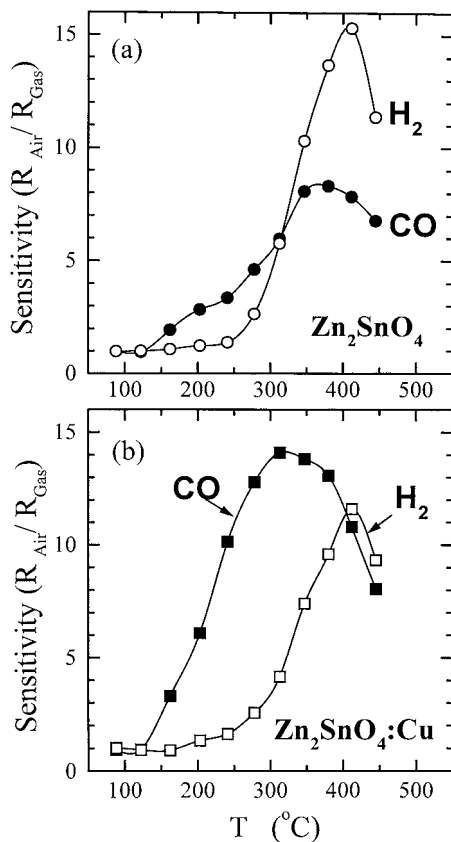Fig. 3. Temperature dependence of the sensitivity of (a) Zn_2SnO_4 and (b) CuO-coated Zn_2SnO_4 (Zn_2SnO_4:Cu) to 200 ppm CO and 200 ppm H_2 gases.
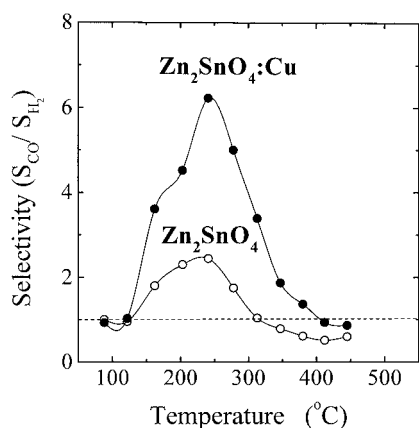

Fig. 4. Temperature dependence of the selectivity of (a) Zn_2SnO_4 and (b) CuO-coated Zn_2SnO_4 (Zn_2SnO_4:Cu) for 200 ppm CO gas (S_{CO}/S_{H_2}).
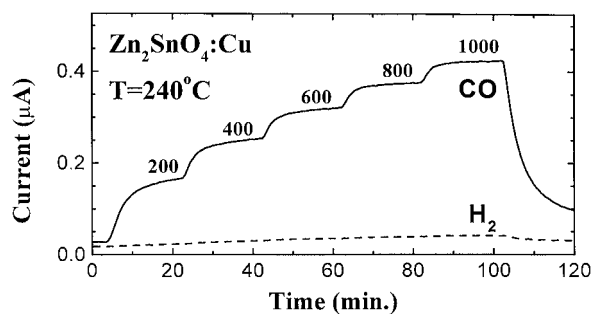

Fig. 5. Selective response of CuO-coated Zn_2SnO_4 (Zn_2SnO_4:Cu) to CO gas against H_2 gas at 240°C. The numbers represent the concentration of reducing gases in ppm. (bias = 5 V, 23% R.H.)

The addition of CuO into Zn_2SnO_4 noticeably changed the gas-sensing properties as shown in Fig. 3(b). The increase of CO sensitivity was accompanied by the shift of sensitivity peak to lower temperature; ~14 at 310°C for Zn_2SnO_4:Cu compared with ~7 at 350°C for uncoated Zn_2SnO_4. However, their CO-gas sensitivities at 450°C changed little. The addition of CuO had a different effect on the H_2 gas sensitivity. The temperature showing maximum sensitivity ($T_{Max} \sim 410$°C) did not change and the sensitivity maximum for H_2 gas was slightly reduced from ~15 for Zn_2SnO_4 to ~12 for Zn_2SnO_4:Cu. Consequently, Zn_2SnO_4:Cu showed much higher selectivity (~6 at 240°C) for CO gas than CuO-free Zn_2SnO_4 (~2.5 at 240°C) as shown in Fig. 4.

Figure 5 shows the response to CO and H_2 gases of Zn_2SnO_4:Cu as the concentration of each reducing gas was increased from 200 ppm to 1000 ppm. The current values was measured while applying 5 Volts in the forward direction, i.e., (−)Pt/ZnO/Zn_2SnO_4/Pt(+). The gas concentration was kept for 20 minutes and raised stepwise while measuring the current every 20 seconds. The increase in the current for Zn_2SnO_4:Cu was negligible up to 1000 ppm H_2 gas concentration.

3.3. Mechanism of the Selective CO Gas Detection of Zn_2SnO_4 and Zn_2SnO_4:Cu

From the results shown above it was revealed that Zn_2SnO_4 shows a selective response to CO gas at low temperature and to H_2 gas at high temperature. Although the CuO addition enhanced the sensitivity and thus the selectivity of Zn_2SnO_4 to CO gas, the basic gas-sensing mechanisms of Zn_2SnO_4 and Zn_2SnO_4:Cu

may be the same. A noticeable feature in the gas-sensing properties of both Zn_2SnO_4 and Zn_2SnO_4:Cu (Figs. 3(a) and (b), respectively) was that the H_2-gas sensitivity curves were narrow in shape and biased toward high temperature. Thus the H_2-gas sensitivities were negligible below $250°C$ while the CO-gas sensitivities were still considerable.

In order to explain the selective CO gas detection of Zn_2SnO_4-based samples, the sensitivity curves of Zn_2SnO_4 were compared with those of SnO_2 [17] and ZnO [20] (5 mol% SnO_2-doped) as shown in Fig. 6. All samples were not coated with CuO. ZnO showed the sensitivity maximum at higher temperature ($\sim410°C$) than SnO_2 ($\sim350°C$) either to CO or to H_2 gas. Both samples showed the higher sensitivity to H_2 than to CO gas at all measurement temperatures and thus no selectivity to CO gas. The temperature for the sensitivity maximum (T_{Max}) of the gas-sensing material is
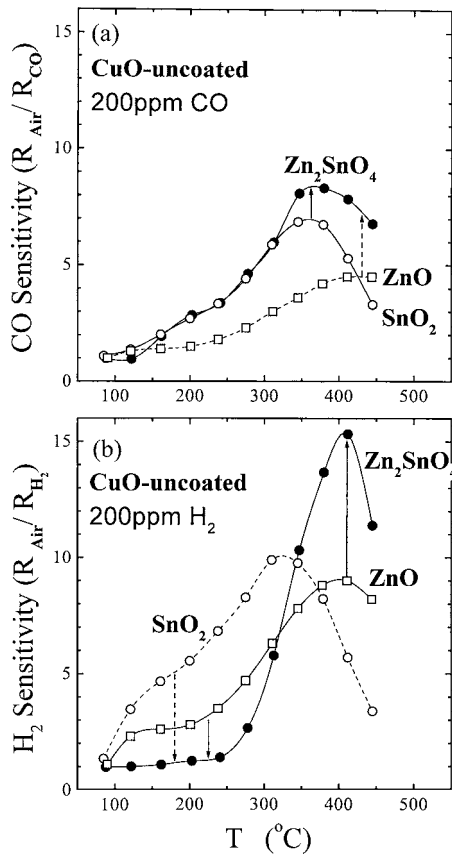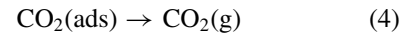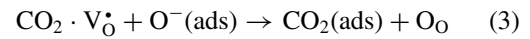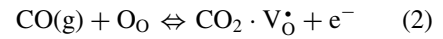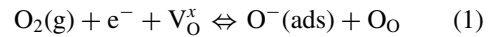

Fig. 6. Temperature dependence of the sensitivity of Zn_2SnO_4 to (a) CO and (b) H_2 gases compared with those of SnO_2 [17] and ZnO:Sn [20].

influenced by many factors such as the catalytic additives [3], reacting gases [3], microstructure [9, 24], and humidity [25]. T_{Max} value for SnO_2, however, is generally lower than that of ZnO [8, 26]. Although we did not plot the sensitivities of other samples for simplicity, SnO_2-based sensor showed T_{Max} about $350–380°C$ despite the different sintering temperature and thus microstructure, and the presence of minor phase (ZnO or Zn_2SnO_4) [8, 10, 27].

Since the selective CO detection of Zn_2SnO_4 was closely related with the difference in T_{Max} values for CO and H_2 gases, it is necessary to discuss why SnO_2 shows the maximum sensitivity at lower temperature than ZnO. It is well known that the adsorbed oxygen groups on SnO_2 oxidize carbon monoxide [28–32]. Infrared (IR) spectroscopy studies showed that the adsorption of CO to form carbonate (CO_3^{-2}) and carboxyl groups (CO_2^-) on the surface of SnO_2 at $\sim400°C$ [28]. Desorption of CO_2 molecules into gas phase returns free electrons thus increases the electrical conductivity of n-type SnO_2.

For ZnO, however, lattice oxygen is known to participate in the oxidation of carbon monoxide by the following elementary steps [33, 34]:

$$O_2(g) + e^- + V_O^x \Leftrightarrow O^-(ads) + O_O \quad (1)$$

$$CO(g) + O_O \Leftrightarrow CO_2 \cdot V_O^{\bullet} + e^- \quad (2)$$

$$CO_2 \cdot V_O^{\bullet} + O^-(ads) \rightarrow CO_2(ads) + O_O \quad (3)$$

$$CO_2(ads) \rightarrow CO_2(g) \quad (4)$$

The oxygen molecules after adsorption occupy the surface site (O^-(ads)) and the bulk lattice site (O_O) (step (1)). The rate-determining step is the step (3) while desorption rate of CO_2 in the reaction (4) is fast. On ZnO surface, CO molecule 'pulls' the lattice oxygen, forming adsorbed CO_2 (step 2) and the chemisorbed oxygen 'pushes' the CO_2 adsorbate into gas phase (step 3) reoccupying the surface lattice site (concerted or push-pull mechanism) [34]. Thus the oxidation of CO occurs even in the absence of O_2 in the gas phase [35]. Since the lattice oxygen of ZnO participates in the oxidation of CO, the high thermal energy is required for ZnO-based gas sensor to detect CO gas. The adsorbed oxygen on SnO_2 surface, however, can easily react with reducing gases due to its relatively low binding energy and high population at low temperature. Consequently, the difference between the sensing temperatures of SnO_2 and ZnO may stem from the
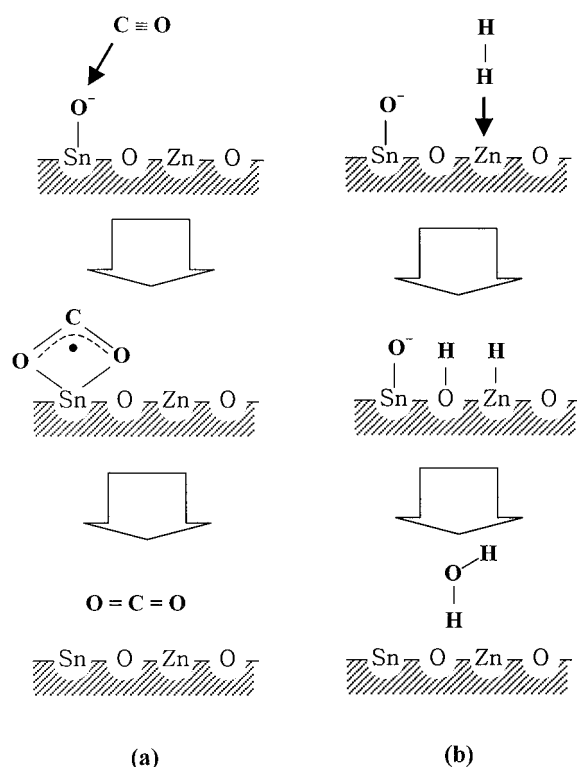
Fig. 7. Possible reaction mechanism of (a) CO and (b) H_2 oxidation on Zn_2SnO_4 surface.

different oxygen species reacting with reducing gas and their bond strength.

It is very interesting that Zn_2SnO_4 shows the sensitivity maximum to CO gas at the nearly same temperature ($\sim$350°C) as SnO_2. However, the temperature for the sensitivity maximum (T_{Max}) to H_2 gas was shown at $\sim$410°C similar to ZnO (Fig. 6). From the results, we propose a possible mechanism of selective detection of CO gas against H_2 gas for Zn_2SnO_4 as shown in Fig. 7. The key in the proposed mechanism is that the reaction routes in CO and H_2 oxidation on the Zn_2SnO_4 surface are different. The oxidation of CO gas on the surface of Zn_2SnO_4 occurs predominantly at low temperature and thus is related to the mechanism of SnO_2 sublattice. CO molecules are selectively adsorbed on Sn–O^- sites forming carboxyl or carbonate group depending upon temperature (Fig. 7(a)). The adsorbate can be desorbed at relatively low temperature due to the weak bond with Sn site.

On the contrary, the H_2 gas-sensing mechanism of Zn_2SnO_4 seems to be mainly determined by that of ZnO sublattice. The oxidation of H_2 on binary oxide

(MO_X) involves the elementary dissociation process of H_2 molecule into M—H and O—H bonding. It was reported that the IR spectra due to Zn—H or Zn—H—Zn (hydridic) and O—H (protonic) bonds appear when ZnO was exposed to H_2 [36, 37]. The adsorption of hydrogen onto Zn site rather than onto Sn site may have resulted in the ZnO-based reaction of hydrogen on Zn_2SnO_4 surface (Fig. 7(b)). Similar to ZnO, the desorption of H_2O from Zn_2SnO_4 needs enough thermal energy due to the relatively strong bond of Zn—H (or Zn—H—Zn) and lattice oxygen. At low temperature, thus, Zn sites present homogeneously on Zn_2SnO_4 surface may work as a poisoning catalyst to the H_2 oxidation. The negligible sensitivity to H_2 gas and thus the high selectivity to CO gas below 240°C can be explained by this mechanism. For clarification, however, further spectroscopic studies on the surface of Zn_2SnO_4 are needed.

The addition of CuO does not seem to make a prominent change in the sensing mechanism of Zn_2SnO_4. The general shapes of sensitivity curve, either for CO gas or for H_2 gas, changed little with CuO addition (Figs. 3(a) and (b)). The magnitude of H_2 gas sensitivity peak decreased with CuO coating while keeping the T_{Max} value. However, the CO gas sensitivity curve moved to lower temperature while the maximum sensitivity value increased. Thus the CuO added into Zn_2SnO_4 acted as a promoter only for CO gas. In the previous report [17], the CuO addition into SnO_2 also lowered T_{Max} for both H_2 and CO gases (from $\sim$350°C to $\sim$200°C), increasing the sensitivity at low temperature. Further addition of ZnO (3 mol%), however, increased T_{Max} only for H_2 gas and thus lowered the H_2 gas sensitivity at low temperature. This suggests that the increased concentration of Zn sites prevented the oxidation of H_2 at low temperature by the similar mechanism shown for Zn_2SnO_4. We also observed that the T_{Max} value for H_2 gas-sensing continuously increased with the increasing content of Zn_2SnO_4 in CuO-coated SnO_2—Zn_2SnO_4 composite [27].

4. Conclusions

The ZnO/Zn_2SnO_4 layered structure was very helpful for the investigation of the electrical and the gas-sensing properties of uncoated and CuO-coated Zn_2SnO_4 due to the ohmic contact between ZnO and Zn_2SnO_4. Zn_2SnO_4 samples, regardless of CuO coating, showed negligible sensitivity to 200 ppm H_2 gas,

on the other hand, considerable sensitivity and thus selectivity for 200 ppm CO gas at low temperature. Although the maximum sensitivity of uncoated Zn_2SnO_4 to CO gas was much less than that to H_2 gas, the selective detection of CO gas was shown below $\sim300°C$. The CuO-coated Zn_2SnO_4 sample showed the enhanced sensitivity and thus the selectivity to CO gas ($S_{CO}/S_{H_2} \sim 6$) from CuO-free sample ($S_{CO}/S_{H_2} \sim 2.5$) at $240°C$, however, the negligible sensitivity even to 1000 ppm H_2 gas. The selectivity of Zn_2SnO_4-based gas sensor to CO gas was obtained mainly due to the difference in the gas sensing temperature between CO and H_2 gases. This suggests that the sensing mechanism for CO gas is different from that for H_2 gas. Thus it was proposed that the CO and the H_2 oxidations are preferred at SnO_2 sublattice at low temperature and at ZnO sublattice at high temperature, respectively. Hydrogen molecules are adsorbed preferentially at Zn sites, which act as a poisoning catalyst to the oxidation of H_2 gas at low temperature.

Acknowledgment

References

1. K. Ihogura and J. Watson, *Stannic Oxide Gas Sensor* (CRC Press, Tokyo, 1993), p. 159.
2. A. Heilig, N. Basan, U. Weimar, and W. Göpel, *Sensors and Actuators B*, **58**, 302 (1999).
3. N. Yamazoe, Y. Kurokawa, and T. Seiyama, *Sensors and Actuators*, **4**, 283 (1983).
4. M. Sauvan and C. Pijolat, *Sensors and Actuators B*, **58**, 295 (1999).
5. Y. Nakamura, A. Ando, T. Tsurutani, O. Okada, M. Miyayama, K. Koumoto, and H. Yanagida, *Chem. Lett.*, 413 (1986).
6. S.T. Jun and G.M. Choi, *Sensors and Actuators B*, **17**, 175 (1994).
7. D.H. Yoon, J.H. Yu, and G.M. Choi, *Sensors and Actuators B*, **46**, 15 (1998).
8. J.H. Yu and G.M. Choi, *Sensors and Actuators B*, **52**, 251 (1998).
9. H.Y. Bae and G.M. Choi, *Sensors and Actuators B*, **55**, 47 (1999).
10. J.H. Yu and G.M. Choi, *Sensors and Actuators B*, **61**, 59 (1999).
11. J.D. Choi and G.M. Choi, *Sensors and Actuators B*, **69**, 120 (2000).
12. J.H. Yu and G.M. Choi, *Sensors and Actuators B*, **72**, 141 (2001).
13. N. Hiratsuka, A. Hosoi, H. Kobayashi, and K. Kakizaki, *J. Ceram. Soc. Jpn (Int. Edition)*, **104**, 1173 (1996).
14. I. Stambolova, K. Konstantinov, M. Khristova, and P. Peshev, *Phys. Stat. Sol. (a)*, **167**, R11 (1998).
15. S. Matsushima, S. Kunitsugu, K. Kobayashi, and G. Okada, *J. Ceram. Soc. Jpn.*, **103**, 302 (1995).
16. H. Nanto, T. Morita, H. Habara, K. Kondo, Y. Douguchi, and T. Minami, *Sensors and Actuators B*, **35/36**, 384 (1996).
17. J.H. Yu and G.M. Choi, *Sensors and Actuators B*, **75**, 56 (2001).
18. J.H. Yu and G.M. Choi, *J. Electrochem. Soc.*, **148**, G307 (2001).
19. Y.S. Shen and T.S. Zhang, *Sensors and Actuators B*, **12**, 5 (1993).
20. J.H. Yu, Ph.D. Thesis, POSTECH, Korea, 2000.
21. M.P. Pechini, U.S. Patent No. 3,330,697 (1967).
22. S.H. Baek, *Sensor Handbook* (Seawha, Korea, 1990), p. 458.
23. S.T. Jun and G.M. Choi, *J. Am. Ceram. Soc.*, **81**, 695 (1998).
24. G.-J. Li, X.-H. Zhang, and S. Kawi, *Sensors and Actuators B*, **60**, 64 (1999).
25. C. Cantalini, M. Faccio, G. Ferri, and M. Pelino, *Sensors and Actuators B*, **18/19**, 437 (1994).
26. H. Yamaura, T. Jinkawa, J. Tamaki, K. Moriya, N. Miura, and N. Yamazoe, *Sensors and Actuators B*, **35/36**, 325 (1996).
27. W.J. Moon, J.H. Yu, and G.M. Choi, *Sensors and Actuators B*, **80**, 21 (2001).
28. M.J. Willet, in *Techniques and Mechanisms in Gas Sensing*, edited by P.T. Moseley, J.O.W. Norris, and D.E. Williams (Adam Hilger, New York, 1991), p. 61.
29. J.F. McAleer, P.T. Moseley, J.O.W. Norris, and D.E. Williams, *J. Chem. Soc. Faraday Trans. 1*, **83**, 1323 (1987).
30. V. Lantto and P. Romppainen, *Surface Science*, **192**, 243 (1987).
31. N. Yamazoe, J. Fuchigami, M. Kishikawa, and T. Seiyama, *Surface Science*, **86**, 335 (1979).
32. P.G. Harrison and A. Guest, *J. Chem. Soc. Faraday Trans. 1*, **85**(8), 1897 (1989).
33. E. Weiss and M. Folman, *J. Chem. Soc. Faraday Trans. 1*, **82**, 2025 (1986).
34. A. Bielanski and J. Haber, *Oxygen in Catalysis* (Marcel Dekker Inc., USA, 1991), p. 132.
35. F. Boccuzzi, A. Chiorino, S. Tsubota, and M. Haruta, *Sensors and Actuators B*, **24/25**, 540 (1995).
36. A. Bielanski and J. Haber, *Oxygen in Catalysis* (Marcel Dekker Inc., USA, 1991), p. 196.
37. F. Boccuzzi, E. Borello, A. Zecchina, A. Bossi, and M. Camia, *Surface Science*, **51**, 150 (1978).